

Magneto-Structural Study of an Oxamato-Bridged Pd^{II}Co^{II} Chain: X-ray Crystallographic Evidence of a Single-Crystal-to-Single-Crystal Phase Transition

Willian X. C. Oliveira,^[a] Marcos A. Ribeiro,^[a] Carlos B. Pinheiro,^[b] Wallace C. Nunes,^[c] Miguel Julve,^[d] Yves Journaux,^[e,f] Humberto O. Stumpf,^[a] and Cynthia L. M. Pereira^{*[a]}

Keywords: Palladium / Cobalt / Magnetic properties / Chain structures / X-ray diffraction

Two new mononuclear oxamato-containing palladium(II) complexes of formula K₂[Pd(opba)]·2H₂O (**1**) and (PPh₄)₂[Pd(opba)]·2H₂O (**2**) and the heterodimetallic palladium(II)–cobalt(II) chain {[Co(H₂O)₂Pd(opba)]·dmsO}_n (**3**) [opba = 1,2-phenylenebis(oxamate), PPh₄⁺ = tetraphenylphosphonium cation and dmsO = dimethyl sulfoxide] have been prepared, and the structures of two of them (compounds **2** and **3**) were determined by X-ray diffraction analysis of single crystals. The structure of **2** consists of discrete anions of [Pd(opba)₂]²⁻ and PPh₄⁺ cations. Each Pd^{II} ion in **2** is surrounded by two oxamate nitrogen atoms and two carboxylate oxygen atoms in a square-planar surrounding. Compound **3** is a neutral chain with regular alternating Pd^{II} and Co^{II} ions, the [Pd(opba)]²⁻ entity acting as a bis(bidentate) ligand towards *trans*-diaquacobalt(II) fragments, and dmsO molecules of

crystallization. Compound **3** exhibits a single-crystal-to-single-crystal phase transition between monoclinic *C*2/*c* (α phase) and triclinic *P* $\bar{1}$ (β phase) space groups. Within the α phase the dmsO molecule of crystallization is disordered, but it becomes ordered below 215 K in the β phase. The ordering process of the dmsO molecule is followed by a reduction in the unit cell volume. The magnetic properties of **3** are barely affected by the structural phase transition, and they indicate an important spin–orbit coupling of the high-spin octahedral Co^{II} ion [$a = 1.245$, $\lambda = -151$ cm⁻¹, $\Delta = 494$ cm⁻¹, the spin Hamiltonian being defined as $\mathbf{H} = -a\lambda\mathbf{LS} + \Delta(\mathbf{L}_z^2 - 2/3) + \beta\mathbf{H}(-a\mathbf{L} + g_e\mathbf{S})$] with an almost negligible intra- [through the diamagnetic square-planar Pd^{II} centre] and interchain antiferromagnetic interactions ($\theta = -0.32$ K).

Introduction

Molecular crystals can experience structural phase transitions as a result of external stimuli, such as temperature, pressure or radiation, while maintaining their structural stability and integrity during the transition process.^[1] Their physical properties (e.g., optical, magnetic or conducting) can then be modulated in a controlled manner, which suggests challenges and opportunities for the development of a crystal engineering approach, referred to as making-crystals-from-crystals and making-crystals-by-design strategies.^[2,3]

Along this line, we reported some years ago the synthesis, crystal structure and magnetic properties of the one-dimensional (1D) compound of formula [CoCu(opba)(dmsO)₃]_n [opba = 1,2-phenylenebis(oxamate), dmsO = dimethyl sulfoxide].^[4] This compound exhibits two crystalline phases characterized by single-crystal X-ray diffraction at two different temperatures, 298 and 100 K. According to birefringence measurements, the structural phase transition takes place at 150 K, and it involves an optical bistability, or optical hysteresis, which suggests a reversible process.^[4] Essentially, the phase transition involves the change from a non-organized to an organized state of the dmsO molecules when the system is cooled. A study of the magnetic properties of [CoCu(opba)(dmsO)₃]_n showed that it behaves as an isolated 1D ferrimagnetic system with a relatively strong intrachain antiferromagnetic coupling (a rough estimate for the magnetic interaction is ca. -30 cm⁻¹).

To better understand the supramolecular and crystal-packing features that can influence the magnetic properties, we reported the related chain compound of formula {[CoCu(opba)]·4H₂O}_n.^[5] Unfortunately, the crystal structure of this compound is still unknown because of the difficulties of obtaining single crystals suitable for X-ray diffraction.

[a] Departamento de Química, Instituto de Ciências Exatas, Universidade Federal de Minas Gerais, 31270-901 Belo Horizonte, MG, Brazil
Fax: +55-31-3409-5700
E-mail: cynthialopes@ufmg.br
Homepage: <http://lattes.cnpq.br/4334534811258685>

[b] Departamento de Física, Instituto de Ciências Exatas, Universidade Federal de Minas Gerais, 1270-901 Belo Horizonte, MG, Brazil

[c] Instituto de Física, Universidade Federal Fluminense, Niterói, RJ 24210-346, Brazil

[d] Departament de Química Inorgànica, Institut de Ciència Molecular (ICMol), Universitat de València, C/ Catedrático José Beltrán 2, 46980 Paterna, Valencia, Spain

[e] Institut Parisien de Chimie Moléculaire, UPMC Univ. Paris 06, Paris 75005, France

[f] CNRS, Institut Parisien de Chimie Moléculaire, UMR 7201, Paris, France

Supporting information for this article is available on the WWW under <http://dx.doi.org/10.1002/ejic.201200831>.

tion. A study of its magnetic properties revealed the occurrence of a glassy behaviour below 3.5 K. This phenomenon was interpreted as being due to the presence of interchain interactions (most likely dipolar and/or through the solvent water molecules) building domains with diameters determined by the magnetic correlation length, as already observed in granular magnetic systems.^[6] In addition, when $\{[\text{CoCu}(\text{opba})] \cdot 4\text{H}_2\text{O}\}_n$ was confined in porous Vycor glass, in which the chains exhibited a limited size, a slow magnetic relaxation occurred accompanied by magnetic hysteresis below the blocked regime temperature ($T < 6$ K). These features are characteristics of single-chain magnets (SCMs).^[7]

From the metallosupramolecular point of view, different transition-metal ions, covalent metal–ligand interactions and intermolecular forces allow “supramolecular-structure–function” correlations to be established that will guide the rational design and synthesis of complexes displaying interesting properties.^[8] Among several examples reported in the literature, structural diversity has led to a wealth of potential applications for magnetism,^[9] molecular recognition,^[10] catalysis^[11] and biological activity.^[12] We have directed our efforts towards the understanding and control of the magnetic properties of molecular architectures obtained through the self-assembly of oxamate-containing building blocks.

Herein we report the synthesis, crystal structure and magnetic properties of the new heterodimetallic chain of formula $\{[\text{Co}(\text{H}_2\text{O})_2\text{Pd}(\text{opba})] \cdot \text{dmso}\}_n$ (**3**), prepared by the reaction of $\text{K}_2[\text{Pd}(\text{opba})] \cdot 2\text{H}_2\text{O}$ (**1**) and cobalt(II) ions in dmso as solvent. The preparation of **1** and its parent $(\text{PPh}_4)_2[\text{Pd}(\text{opba})] \cdot 2\text{H}_2\text{O}$ (**2**) derivative (PPh_4^+ = tetraphenylphosphonium cation) as well as the crystal structure of **2** are also reported. Interestingly, **3** exhibits thermal polymorphism, a phenomenon previously observed in $[\text{CoCu}(\text{opba}) \cdot (\text{dmso})_3]_n$. The preparation of single crystals of **3** provides us with the opportunity to observe a structural phase transition [monoclinic (α) \rightarrow triclinic (β)], determine the original crystal structure of the α phase and re-examine that of the β phase by using the single-crystal X-ray diffraction data. Variable-temperature magnetic susceptibility measurements on polycrystalline samples of **3** allowed us to evaluate the magnetic contribution arising from only the anisotropic six-coordinate Co^{II} ions in the chain structure, the square-planar Pd^{II} cation being diamagnetic.

Results and Discussion

Synthesis and General Characterization

The mononuclear palladium(II) complex **1** was prepared by treating the $\text{K}_2[\text{PdCl}_4]$ salt with the $\text{Et}_2\text{H}_2\text{opba}$ proligand in basic (KOH) aqueous solutions. The subsequent metathesis with PPh_4Cl afforded the parent tetraphenylphosphonium derivative **2**. The chain compound **3** was obtained by the treatment of **1** with $[\text{Co}(\text{H}_2\text{O})_6]\text{Cl}_2$ in dmso. The analytical data are consistent with the formation of a heterodimetallic palladium(II)–cobalt(II) compound in a 1:1 $\text{Co}^{\text{II}}/\text{Pd}^{\text{II}}$ molar ratio. All products are stable in air at

room temperature. Complex **1** is soluble in polar solvents such as water and dimethyl sulfoxide but is insoluble in diethyl ether, methanol and ethanol. Complex **2** is soluble in water and insoluble in dimethyl sulfoxide, ethanol, methanol and diethyl ether. Finally, compound **3** is insoluble in water, dimethyl sulfoxide, ethanol, methanol and diethyl ether.

The thermogravimetric/differential thermal analysis (TGA/DTA) data for **1–3** are given in the Supporting Information (Figures S1–S3). The TGA curve of **1** under N_2 shows a first mass loss in the temperature range of 24–193 °C, which has been attributed to the departure of two water molecules (found 9.0%; calcd. 7.7%), and it corresponds to the endothermic peaks at 28, 50, 108 and 155 °C in the DTA curve (Figure S1). At least three consecutive mass losses can be observed above 193 °C, which correspond to the exothermic peak at 375 °C, and they have been attributed to the thermal decomposition of the oxamate ligand.^[13] The amount of residue (found 42.49%; calcd. 42.79%) at 750 °C is in agreement with the formation of equimolar amounts of Pd and K_2O as the final products.

The TGA curve of **2** under N_2 shows that the anhydrous compound is stable up to 225 °C (Figure S2). Above this temperature, thermal decomposition occurs in three steps within the temperature ranges of 224–322, 322–610 and 610–750 °C, the losses of mass amounting to 6.4, 76.5 and 13.48%, respectively. The DTA curve shows two exothermic peaks at 285 and 471 °C, which have been attributed to the thermal decomposition and oxidation of organic matter, respectively.^[13]

The simultaneous TGA/DTA curves for compound **3** under N_2 (Figure S3) show the first mass loss in the temperature range 24–122 °C, corresponding to an endothermic peak at 107 °C, which is due to dehydration with the loss of two water molecules (found 6.70%; calcd. 6.83%). The second mass loss occurs in the range 216–370 °C (endothermic shoulder at 342 °C), most likely due to the removal of the free dmso (found 15.82%; calcd. 14.82%). The thermal decomposition of the organic ligand occurs in two consecutive steps in the temperature ranges of 370–505 and 505–750 °C (exothermic peak at 362 °C). At 750 °C, the final residue of 35.24% essentially contains equimolar amounts of Pd and CoO (calcd. 34.42%).

The IR spectra of **1–3** are in agreement with the proposed molecular formulae, confirmed by the crystallographic data. The vibrational spectrum of **1** shows a broad band at 3390 cm^{-1} , which has been attributed to the $\nu(\text{OH})$ stretching mode and indicates the presence of water molecules, in agreement with the TGA curve. The most important aspect in the IR spectrum of this complex is, however, the lack of peaks assigned to $\nu(\text{NH})$ at 3259 cm^{-1} and the shifting of the $\nu(\text{CO})$ vibrations of the free ligand (originally at 1762, 1740 and 1690 cm^{-1}) to lower wavenumbers in **1** (ca. 1659 and 1630 cm^{-1}). This strongly suggests the coordination of the palladium(II) ion to the nitrogen and oxygen atoms of the oxamate ligand in a square-planar geometry. Compound **2** presents a very similar spectrum to **1**, the major differences consisting of the bands assigned to

the phenyl rings from the tetraphenylphosphonium cations at 3064, 1614, 1410 and 724 cm⁻¹ and the strong absorption peak at 1110 cm⁻¹ assigned to the P–C stretching vibration. The weak peaks observed at 541 and 449 cm⁻¹ for **1** and at 526 and 442 cm⁻¹ for **2** have tentatively been assigned to $\nu(\text{Pd–O})$ and $\nu(\text{Pd–N})$ vibrations, respectively.^[14]

The IR spectrum of **3** shows a broad absorption band at 3396 cm⁻¹ attributed to $\nu(\text{OH})$, which confirms the presence of water molecules. In addition, the most important aspects in the spectrum of the chain compound are the shift towards lower wavenumbers of the bands assigned to $\nu(\text{CO})$ (originally at 1659 and 1630 cm⁻¹ in the spectrum of **1** to 1606 and 1570 cm⁻¹ in the spectrum of compound **3**) and a medium-intensity band at 1010 cm⁻¹ attributed to the $\nu(\text{SO})$ stretching mode of the dmsu molecule. Bands at 584, 550 and 474 cm⁻¹ most likely correspond to the $\nu(\text{Co–O})$, $\nu(\text{Pd–O})$ and $\nu(\text{Pd–N})$ vibrations, respectively. All these facts reinforce the coordination of oxygen atoms to Co^{II} ions, confirmed by the crystallographic data.

X-ray Structures of **2** and **3**

X-ray diffraction experiments were carried out at 273(2) K on **2** and at 293(2) and 150(2) K on **3**. A summary of the crystallographic data and structure refinements are given in Table 1, and selected bond lengths and angles for **2** and **3** are shown in Tables 2 and 3, respectively. The X-ray powder diffraction patterns of **2** and the α phase of **3** are shown in Figures S4 and S5 in the Supporting Information,

respectively. The experimental patterns of the polycrystalline samples agree with the results obtained by single-crystal X-ray measurements, which indicates that they have the same structures.

The crystal structure of **2** consists of discrete palladium(II) complex anions, $[\text{Pd}(\text{opba})]^{2-}$, tetraphenylphosphonium cations and water molecules of crystallization. A perspective view of the mononuclear entity with the atom-numbering scheme is depicted in Figure 1. The palladium(II) ion is coordinated to two deprotonated amide nitrogen atoms and two carboxylate oxygen atoms from the opba ligand in a slightly distorted square-planar geometry. The metal atom is located almost in the plane defined by the N₂O₂ set of coordinating atoms. The fully deprotonated opba⁴⁻ ligand adopts a tetradentate coordination mode forming three five-membered chelate rings around the palladium(II) ion. The bite angles subtended at the metal ion by the opba ligand are smaller than the ideal value of 90° [N1–Pd1–N2 84.95(13)°, N1–Pd1–O4 82.75(12)° and N2–Pd1–O3 82.83(13)°], but they are in agreement with those reported for the parent compound Na[Pd(Hpba)]·2H₂O [H₄pba = 1,3-propylenebis(oxamic acid)].^[15] The outer bond angle in **2** [O3–Pd1–O4 109.49(13)°] is, however, larger than that observed in Na[Pd(Hpba)]·2H₂O [99.6(2)°], but similar to that in the analogous copper(II) complex, (PPh₄)₂[Pd(opba)]·2H₂O [106.1(3)°].^[16] all three being larger than the ideal value of 90°. This is a unique feature of planar complexes with a fused 5–5–5 ring chelate system: three of the bond angles at the metal atom are roughly

Table 1. Crystal data and structure refinement for **2** and **3**.^[a,b]

	2	3 (α phase)	3 (β phase)
Empirical formula	C ₅₆ H ₄₄ N ₂ O ₆ PPd	C ₁₂ H ₁₄ N ₂ O ₉ SCoPd	C ₁₂ H ₁₄ N ₂ O ₉ SCoPd
M_r [g mol ⁻¹]	973.24	527.67	527.67
Crystal system	monoclinic	monoclinic	triclinic
Space group	$P2_1$	$C2/c$	$P\bar{1}$
Temperature [K]	273	293	150
a [Å]	10.3985(2)	10.720(2)	10.718(2)
b [Å]	17.0397(3)	23.189(5)	12.514(3)
c [Å]	13.3902(3)	7.2630(15)	7.1932(14)
α [°]	90	90	86.34 (3)
β [°]	96.837(2)	103.74(3)	104.29(3)
γ [°]	90	90	113.08(3)
V [Å ³]	2357.11(8)	1753.8(6)	859.5(3)
Z	2	4	2
T [K]	293(2)	293(2)	150(2)
λ [Å]	0.71073	0.71073	1.5418
$\rho_{\text{calcd.}}$ [g cm ⁻³]	1.371	1.998	2.038
μ [mm ⁻¹]	0.513	2.12	17.62
$F(000)$	1060	952	522
Crystal size	0.53 × 0.29 × 0.19	0.19 × 0.09 × 0.06	0.18 × 0.08 × 0.07
θ range [°]	2.8–29.5	1.8–26.4	3.8–66.7
h	–13 to 12	–13 to 13	–12 to 12
k	–21 to 21	–28 to 28	–14 to 14
l	–16 to 16	–9 to 9	–8 to 8
Reflections collected	34285	19078	31351
Independent reflections (R_{int})	9606 (0.38)	1790 (0.1)	5658 (0.069)
$R_1^{\text{[a]}}$ [$I > 2\sigma(I)$]	0.043	0.047	0.101
$wR_2^{\text{[b]}}$ [$I > 2\sigma(I)$]	0.099	0.137	0.228
$S^{\text{[c]}}$	1.081	1.10	1.37
Residuals [e Å ⁻³]	2.71, –0.36	1.75, –0.92	3.4, –1.41

[a] $R_1 = \Sigma(|F_o| - |F_c|)/\Sigma|F_o|$. [b] $wR_2 = [\Sigma w(|F_o| - |F_c|)^2/\Sigma w|F_o|^2]^{1/2}$. [c] $S = w = 1/[\sigma^2 F_o^2 + (0.0766P)^2 + 9.5127P]$, in which $P = (F_o^2 + 2F_c^2)/3$.

equal, and the fourth one, being less constrained, is appreciably larger. The Pd–N_{amidate} bonds are significantly shorter than the Pd–O_{carboxylate} bonds (see Table 2). These values are also slightly larger than those observed for (PPh₄)₂·[Pd(opba)]·2H₂O [Cu–N 1.89–1.93 Å and Cu–O 1.93–1.97 Å].^[16] The trapezoidal unit composed of the N₂O₂ donor set around the palladium(II) ion exhibits O3···O4 and N1···N2 distances of 3.355 and 2.604 Å, respectively {to be compared with 3.093 and 2.531 Å in (PPh₄)₂·[Pd(opba)]·2H₂O},^[16] the lengthening in the palladium derivative being as expected because of the larger size of Pd^{II} relative to the Cu^{II} ion.

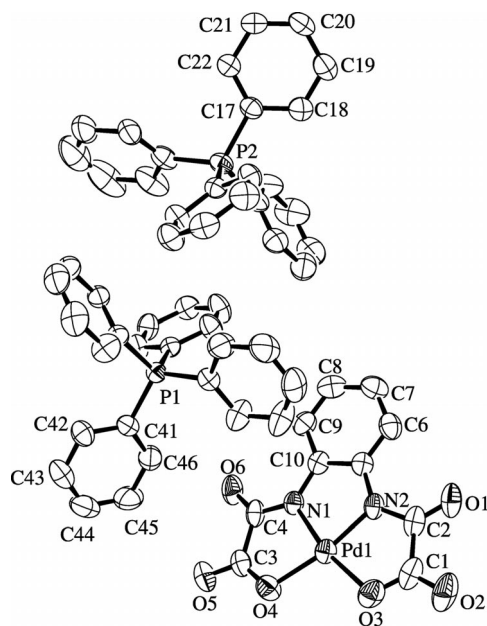


Figure 1. ORTEP[®] drawing of **2** showing the atom-numbering scheme. Thermal ellipsoids are drawn at the 50% probability level. Hydrogen atoms have been omitted for clarity.

Table 2. Selected bond lengths [Å] and angles [°] for **2**.^[a]

Pd1–N1	1.923(3)	N1–Pd1–N2	84.95(13)
Pd1–N2	1.933(3)	N1–Pd1–O4	82.75(12)
Pd1–O3	2.051(3)	N2–Pd1–O3	82.83(13)
Pd1–O4	2.058(3)	O3–Pd1–O4	109.49(13)

[a] Estimated standard deviations are given in parentheses.

From the supramolecular point of view, the presence of PPh₄⁺ cations was fundamental to obtaining single crystals of compound **2** due to the intermolecular phenyl–phenyl interaction, as has been observed for several systems.^[17] In the crystal of **2**, each pair of PPh₄⁺ cations associate according to the most prevalent supramolecular motif, namely the sextuple phenyl embrace (SPE), which involves three phenyl atoms in each molecule interleaving with three from the other one in the interpenetration domain. This configuration is described as an edge-to-face interaction in which the rings are steeply canted such that two hydrogen atoms on the edge of one ring are directed towards the carbon atoms of the other one, as depicted in Figure 1.^[17a] The fourth phenyl group in each PPh₄⁺ points away from the

interaction domain, and the C–P vectors situated on the two P atoms are close to *trans* colinearity [C41–P1···P2 and C17–P2···P1 are 168.64(13) and 166.55(12)°, respectively]. The distance between P1···P2 is 6.444(12) Å, in agreement with that expected for SPE motifs.^[17a,17b]

The crystal packing of **2** (Figure S6) demonstrates that mutually attractive interactions between the PPh₄⁺ cations occur through a zigzag infinite sextuple phenyl embrace (ZZISPE).^[17b] Each PPh₄⁺ cation presents three phenyl rings interacting with each of its neighbours; as a consequence three are involved in six edge-to-face interactions between each pair of cations related by a centre of inversion.^[17] The zigzag geometry occurs due to the tetrahedral disposition of the phenyl groups at P, and the P···P···P angles are 107.65°, which is approximately the value of the tetrahedral angle. The most important feature of this array is the coplanarity of all the P atoms, following the requirements of the SPE. The predominant crystal packing arrangement consists of stacks of anions [Pd(opba)]²⁻ between and parallel to chains of ZZISPE that are not able to participate in phenyl embraces. The crystal structure of **2** is free of the crystallographic disorder shown by the cations, which indicates the significance of these extended multiple phenyl embraces.^[17c]

The structures of the α and β phases of **3** are shown in Figure 2. At higher temperatures (293 K), compound **3** crystallizes in the monoclinic system, space group *C2/c* (α phase), whereas at lower temperatures (150 K) it crystallizes in the triclinic system, space group *P* $\bar{1}$ (β phase). Therefore, the transformation involves a crystallographic triclinic \rightarrow monoclinic phase transition, which is ultimately related to the disorder–order of the crystallization dmsol molecule.

In both phases, the structure of **3** consists of neutral linear chains running along the crystallographic *c* axis with regular alternating Pd^{II} and Co^{II} ions bridged by oxamate groups. Within each chain, the bis(oxamato)palladate(II) entity acts as a bis(bidentate) ligand through the two *cis*-carbonyl oxygen atoms. The geometry around the palladium(II) ion is approximately square-planar, PdN₂O₂, with two amidate nitrogen atoms and two carboxylate oxygen atoms from the fully deprotonated opba⁴⁻ group in the basal plane. The bond lengths around the Pd^{II} ion and the corresponding bite angles are quite similar in both phases (Table 3). The values of the dihedral angle between the basal plane of palladium(II) and the mean plane of the oxamate group are 1.74 (α) and 2.59° (β). Each cobalt(II) ion in the two structures is six-coordinate with two *trans*-coordinated water molecules and four carbonyl oxygen atoms from the oxamate group building a somewhat distorted octahedral surrounding. The bond lengths around the cobalt atom in both phases are very similar (Table 3), and they are close to those observed for the high-spin Co^{II} ion in the oxamato-bridged heterodimetallic cobalt(II)–copper(II) chains [CoCu(opba)(dmsol)₃]_n and {[CoCu(2,4,6-tmpa)₂(H₂O)₂·4H₂O]_n [2,4,6-tmpa = *N*-(2,4,6-trimethylphenyl)oxamate].^[4,7b] The intrachain Pd1···Co1 separations in the α [5.383(11) Å] and β phases [5.384(2) Å] are practically identical and are in agreement with those previously reported

= 4.967(4) Å in the β phase [symmetry codes: (iv) $x, -y, z + 1/2$; (vii) $2 - x, -1 - y, -1 - z$]. These values are smaller than those observed in $\{[\text{CoCu}(2,4,6\text{-tmpa})_2(\text{H}_2\text{O})_2] \cdot 4\text{H}_2\text{O}\}_n$ [$\text{Cu} \cdots \text{Cu} = \text{Co} \cdots \text{Co} = 8.702$ Å] and $[\text{CoCu}(\text{opba})(\text{dmsO})_3]_n$ [$\text{Cu} \cdots \text{Cu} = 9.614(1)$ and $9.424(1)$ Å]. The shortest interchain Pd \cdots Co separations are Pd \cdots Co^{viii} = 6.925(18) Å in the α phase and Pd \cdots Co^{ix} = 6.895(2) Å in the β phase [symmetry codes: (viii) $x, -y, z + 1/2$; (ix) $2 - x, -1 - y, -1 - z$], which shows that the chains in both phases have practically the same structure. These values are slightly larger than the corresponding ones observed in the analogous Cu^{II}Co^{II} chains (Cu \cdots Co = 5.310 Å for $\{[\text{CoCu}(2,4,6\text{-tmpa})_2(\text{H}_2\text{O})_2] \cdot 4\text{H}_2\text{O}\}_n$ and Cu \cdots Co 5.336 and 5.305 Å for $[\text{CoCu}(\text{opba})(\text{dmsO})_3]_n$). Finally, it is interesting to note that the Pd^{II} ions from two adjacent chains in compound **3** are situated almost in the middle of the aromatic ring of the opba ligand, the distances between the plane of the aromatic ring and the Pd^{II} ion being 3.478(7) in the α phase and 3.405(9) Å in the β phase.

Magnetic Properties of **3**

The temperature dependence of the $\chi_M T$ product for **3** (χ_M being the magnetic susceptibility per mol of Co^{II}) is shown in Figure 4. At room temperature, $\chi_M T$ is equal to 3.0 cm³ mol⁻¹ K, a value that is close to the typical one for an isolated Co^{II} ion. This value was expected, because the Pd^{II} ion in a square-planar geometry is diamagnetic. Then, the magnetic behaviour exhibited by compound **3** is exclusively a result of the Co^{II} ion. Upon cooling, a slight bump appears at 215 K [Figure 4(b)], which is also observed in the warming mode, supporting the reversibility of the phenomenon. This can be related to the occurrence of a reversible structural phase transition that seems to exert a negligible influence on the magnetic behaviour. In this respect, previous reports have indicated that crystallographic phase transitions can result in either significant or slight modifications of the magnetic curves.^[18,19] This is not unexpected, because the coordination sphere of cobalt(II) is only slightly modified by the phase transition. On lowering the temperature, the $\chi_M T$ value steadily decreases to reach a region, between 14 and 12 K, in which the value of $\chi_M T$ does not decrease much. The origin of this “plateau” is unclear and may be related to another structural change at low temperature. Below 10 K, the decrease in $\chi_M T$ is steeper and finally a value of 1.52 cm³ K mol⁻¹ is attained at 4 K. This value is slightly below that expected for a magnetically isolated Co^{II} ion at low temperature (1.75 cm³ K mol⁻¹) considering an effective spin S_{Co} of 1/2 and a Landé factor g of around 4.3.^[20,21] No maximum of the magnetic susceptibility was observed in the χ_M versus T plot. The decrease in $\chi_M T$ from room temperature to 14 K can be attributed to the depopulation of the higher energy levels as a result of the spin-orbit interaction of the octahedral high-spin Co^{II} ions. Below this temperature there is an unexplained anomaly down to 10 K, and the final decrease in $\chi_M T$ is probably due to the effect of a small antiferromagnetic interaction between Co^{II} ions.

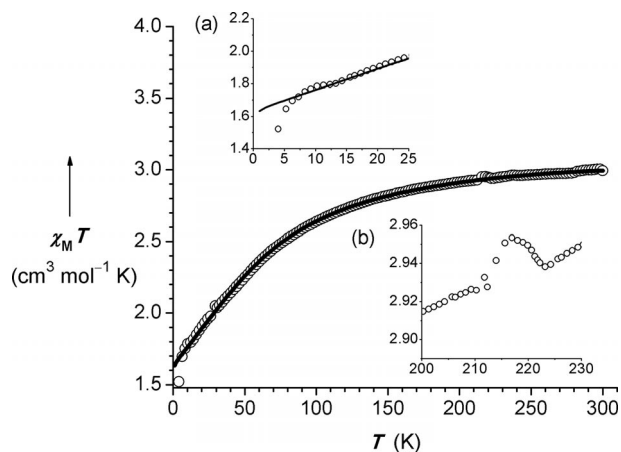


Figure 4. $\chi_M T$ vs. T plot for **3** under an applied d.c. field of 1 kG. The solid line corresponds to the best-fit curve. Inset (a) shows an enlargement of the low-temperature region. Inset (b) details the bump in the $\chi_M T$ vs. T plot showing a structural phase transition at around 215 K.

Bearing in mind that we are dealing with a quasi-magnetically isolated six-coordinate high-spin cobalt(II) ion, we analysed the magnetic susceptibility data of **3** by using the following Hamiltonian [Equation (1)].

$$H = -a\lambda LS + \Delta(L_z^2 - 2/3) + \beta H(-aL + g_e S) \quad (1)$$

The first term in this Hamiltonian corresponds to the spin-orbit coupling effects, with λ being the spin-orbit coupling constant and a defined as $a = A\kappa$, with A being a parameter that depends on the strength of the crystal field and κ being the orbital reduction factor arising from the covalent character of bonds involving metal and ligands. The value of A varies between 3/2 and 1 for a weak crystal field to a strong crystal field, respectively, and typical values of κ for six-coordinate high-spin cobalt(II) ions are in the range 0.70–0.95.^[22] The second term in this Hamiltonian is the one-centre operator responsible for the axial distortion of the six-coordinate Co^{II} ion, with Δ being the energy gap between the singlet 4A_2 and doublet 4E levels arising from the splitting of the $^4T_{1g}$ ground state under an axial distortion. The last term represents the Zeeman interaction.

Setting the parameter A to 3/2 and adding a Curie-Weiss law term (θ) to take into account the inter- and intrachain antiferromagnetic interactions at low temperature, the least-squares fit of the experimental data of **3** using a full diagonalization of the Hamiltonian matrix performed in the 300–4 K temperature range led to $\lambda = -151$ cm⁻¹, $\Delta = 494$ cm⁻¹, $\kappa = 0.90$ and $\theta = -0.32$ K with $R = 8 \times 10^{-6}$ (R is the agreement factor defined as $R = \Sigma[(\chi_M T)^{\text{calcd.}} - (\chi_M T)^{\text{obs.}}]^2 / [(\chi_M T)^{\text{obs.}}]^2$). The theoretical curve (solid line in Figure 4) reproduces extremely well the magnetic data in the 300–14 K temperature range and the values of a , λ and Δ lie within the range of those reported for other octahedral cobalt(II) complexes.^[22] Below 14 K, the experimental points deviate from the theoretical curve for isolated Co^{II} ions without the Curie-Weiss term [Figure 4(a)] as a result of magnetic interactions between the cobalt(II) ions. The ex-

perimental values are lower than the calculated curve for isolated Co^{II} ions showing that this interaction is antiferromagnetic. It is impossible to know the main interaction responsible for this behaviour, whether it is due to the interaction between the cobalt(II) ions belonging to adjacent chains or between the Co^{II} ions through the [Pd(opba)]²⁻ complex or to the sum of both intra- and intermolecular interactions. Despite the very long distances between the cobalt ions within the chain [10.718(4) and 10.720(3) Å, symmetry code: $x + 1, y, z$ for both phases], probably the right hypothesis is the final one due to the presence of the HOMOs of the [Pd(opba)]²⁻ complex, able to transmit the electronic interaction. Examples of interactions between first-row transition-metal ions through diamagnetic ions are known.^[23]

The field dependence (H) of the magnetization (M) at 2.8 K and the magnetization calculated by using the best-fit parameters from the fit of the $\chi_M T$ versus T plot for a polycrystalline sample of **3** are depicted in Figure 5. The agreement is reasonably good, except in the low-field region in which the experimental points are below the calculated curve. This behaviour confirms the existence of some antiferromagnetic interaction between the cobalt(II) ions. At 2.8 K, the magnetic field has to overcome this interaction in order to recover the behaviour of isolated cobalt ions. The saturation value of the magnetization at 6 T is 2.1 BM per Co^{II} ion. Owing to the fact that only the ground Kramers' doublet is populated at such a low temperature, a value of $g = M_{\text{sat.}}/S_{\text{eff.}} = 2.1 \times 2 = 4.2$ is then calculated. As $g = (10 + 2a)/3$, the derived value of a is 1.3. This value is in good agreement with that of 1.245 obtained from the fit of the magnetic susceptibility data.

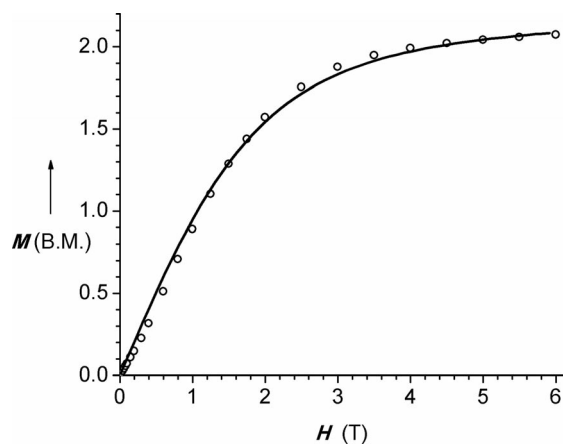


Figure 5. M vs. H plot for **3** at 2.8 K. The solid-line curve was calculated with the best parameters obtained from the best-fit of the $\chi_M T$ vs. T plot.

Conclusions

One of the outcomes of this work is the description for the first time of an oxamato-bridged palladium(II)–cobalt(II) chain compound in which the diamagnetic nature of the square-planar Pd^{II} ion allows evaluation of the indi-

vidual contribution of the Co^{II} ions to the magnetic properties of 1D magnetic systems. According to our results, the system can be considered quasi-magnetically isolated, because the Co^{II} ions are far away from each other in terms of both the intra- and interchain metal–metal separations. More importantly, a structural monoclinic \rightarrow triclinic phase transition was also identified during cooling, as previously reported for the related oxamato-bridged copper(II)–cobalt(II) chain compound [CoCu(opba)(dmsO)₃]_n. The ordering of the dmsO molecule of crystallization is responsible for the transition. The magnetic data in the warming mode also reflect this phase transition, and they support its reversible character.

Finally, the ability of oxamate-based palladium(II) complexes to act as catalysts in processes such as the hydrogenation of organic substrates, envisaging the preparation of various fine chemicals,^[11b] as well as the tuning of niobia catalyst properties to the interests of the petrochemical industry,^[24] are perspectives of this work.

Experimental Section

General: All reactants were of analytical grade and were used without further purification. The Et₂H₂opba proligand was prepared according to the same procedure as described elsewhere.^[25] Elemental analysis (C, H and N) was performed with a Perkin–Elmer 2400 analyser. Atomic absorption spectrophotometry for Co was performed with a Hitachi Z-8200 Polarized Atomic Absorption Spectrophotometer. Infrared spectra were recorded with a Perkin–Elmer 882 spectrophotometer in the range 4000 and 400 cm⁻¹ by using KBr pellets. Thermogravimetric analysis (TG/DTA) data were collected with a Shimadzu TG/DTA 60 instrument by using 2.0 mg of the samples packed into an alumina crucible. Samples were heated at 10 °C min⁻¹ from room temperature to 750 °C in a flow of nitrogen (flow rate 200 cm³ min⁻¹) and oxygen (flow rate 100 cm³ min⁻¹). ¹H NMR spectra were obtained at room temperature using a Bruker DRX-400 Avance (400 MHz) spectrometer using deuterium oxide (D₂O) as the solvent and tetramethylsilane (TMS) as internal reference. X-ray powder diffraction patterns were obtained by using a Rigaku/Geirgflex diffractometer at room temperature. Data were collected in the Bragg/Brentano mode (1 ° s⁻¹) using monochromatic Cu- K_{α} radiation (see Figures S4 and S5 in the Supporting Information). The d.c. magnetic measurements were performed with a magnetometer SQUID Cryogenic S600 instrument. The diamagnetic corrections for the constituent atoms were estimated from Pascal's tables and corrections for the sample holder were also applied.

Preparation of the Compounds

K₂[Pd(opba)]·2H₂O (1): K₂[PdCl₄] (0.327 g, 1.0 mmol) was dissolved in water (10 mL) and slowly added to an aqueous solution (10 mL) of Et₂H₂opba (0.308 g, 1.0 mmol) previously hydrolysed with KOH (0.264 g, 4.0 mmol) at 40 °C. The resulting solution was stirred at 40 °C for 24 h, then filtered, and the volume was reduced to a third under vacuum. The greenish-yellow solid that separated was filtered off, washed with acetone and dried under vacuum. Yield: 450 mg (70%). C₁₀H₈K₂N₂O₈Pd (468.8): calcd. C 25.62, H 1.87, N 5.98; found C 25.44, H 1.95, N 5.88. IR (KBr): $\tilde{\nu} = 3389, 2961, 2921, 1659, 1630, 1575, 1472, 1456, 1420, 1385, 874, 774, 741, 583, 541, 449$ cm⁻¹. Main signals in ¹H NMR (D₂O): $\delta = 6.87$ (dd, 1 H, Ph-H₃), 7.96 (dd, 1 H, Ph-H₄) ppm.

(PPh₄)₂[Pd(opba)] (2): PPh₄Cl (0.820 g, 2.0 mmol) dissolved in water (10 mL) was added to an aqueous solution (40 mL) of K₂[Pd(opba)]·2H₂O (0.820 g, 2.0 mmol) under continuous stirring. The mixture was allowed to concentrate at room temperature, and yellow crystals of **2** suitable for X-ray analysis appeared after 1 month. They were collected by filtration, washed with cold water and dried in air. Yield: 671 mg (65%). C₅₈H₄₄N₂O₆P₂Pd (1033.35): calcd. C 67.41, H 4.29, N 2.71; found C 66.89, H 3.95, N 2.74. IR (KBr): $\tilde{\nu}$ = 3450, 3064, 2924, 2854, 1656, 1638, 1614, 1570, 1470, 1438, 1410, 1384, 1280, 1230, 1110, 1038, 996, 870, 752, 538, 526, 442 cm⁻¹.

Synthesis of {[Co(H₂O)₂{Pd(opba)}]·dmsO}_n (3): An H₂O/dmsO (1:1, v/v, 20 mL) mixture was poured into a glass test-tube containing K₂[Pd(opba)]·2H₂O (0.030 g, 0.64 mmol). Then an aqueous solution (2 mL) of CoCl₂·6H₂O (0.015 g, 0.064 mmol) was carefully added dropwise, and the contents of the tube was covered with Parafilm®. X-ray quality crystals of **3** were obtained after standing at room temperature for 1 month. They were collected by filtration, washed with minimum amounts of cold water and dried in air. Yield: 26.5 mg (83%). C₁₂H₁₄CoN₂O₉PdS (527.67): calcd. C 27.31, H 2.67, N 5.31, Co 10.59; found C 27.35, H 2.28, N 5.61, Co 11.17. IR (KBr): $\tilde{\nu}$ = 3396, 1606, 1570, 1468, 1420, 1344, 1276, 1010, 956, 882, 752, 584, 550, 474, 448 cm⁻¹.

Crystal Structure Determinations: Single crystals of compounds **2** and **3** were mounted on polyamide sample holders and used for data collection. X-ray diffraction measurements were performed with an Oxford Diffraction GEMINI-Ultra diffractometer using graphite-monochromated Mo-K α radiation (λ = 0.71069 Å) at 293(2) K (**2** and **3**) and Cu-K α radiation (λ = 1.5418 Å) at 150(2) K (**3**, β phase). Data integration and scaling of the reflections were performed with the CRYCALIS suite.^[26] Final unit cell parameters were based on the fitting of all reflection positions. The structures were solved by direct methods using the program SUPERFLIP^[27] and refined by full-matrix least-squares techniques against F^2 by using SHELXL-97.^[28] Positional and anisotropic atomic displacement parameters were refined for all non-hydrogen atoms. The dmsO molecules in the structure of **3** were found to be disordered at 293 K and were refined with split atomic positions over the two-fold axis. All hydrogen atoms were located in difference maps and included as fixed contributions riding on the attached atoms. The criteria for a satisfactory complete analysis were the ratios of rms shift to standard deviations less than 0.001 and no significant features in final difference maps. Molecular graphics were produced with the ORTEP programme.^[29] A summary of the crystal data, experimental details and refinement results is given in Table 1. CCDC-892812 (for **2**), -892814 [for **3** (α phase)] and -892813 [for **3** (β phase)] contain the supplementary crystallographic data for this paper. These data can be obtained free of charge from The Cambridge Crystallographic Data Centre via www.ccdc.cam.ac.uk/data_request/cif.

Supporting Information (see footnote on the first page of this article): TG/DTA curves and X-ray diffraction patterns for **1**, **2** and **3** (α phase), and also ORTEP® drawings showing the crystal packing of **2** and **3**.

Acknowledgments

The authors thank the Conselho Nacional de Desenvolvimento Científico e Tecnológico (CNPq), the Fundação de Amparo à Pesquisa do Estado de Minas Gerais (FAPEMIG), the Coordenação de Aperfeiçoamento de Pessoal de Nível Superior (CAPES) and the Ministerio Español de Ciencia e Innovación (Project CTQ2010-

15364) for financial support and grants. The authors are also grateful to the graduate student I. F. Teixeira, to Professors M. I. Yoshida and R. M. Lago, both from the Universidade Federal de Minas Gerais (Brazil), for TG/DTA curves and to Professor M. A. Novak (Universidade Federal do Rio de Janeiro, Brazil) for allowing us to use the magnetometer. Thanks are also extended to Msc. A. de Melo Moreira (Departamento de Física, Laboratório de Cristalografia, Universidade Federal de Minas Gerais) for X-ray diffraction patterns and Dr. R. Ruiz-García and Prof. Dr. F. Lloret, both from the Universitat de València, for fruitful discussions.

- [1] M. A. García-Garibay, *Angew. Chem.* **2007**, *119*, 9103; *Angew. Chem. Int. Ed.* **2007**, *46*, 8945–8947, and references therein.
- [2] D. Braga, F. Grepioni, *Chem. Commun.* **2005**, *29*, 3635–3645.
- [3] D. Braga, *Chem. Commun.* **2003**, *22*, 2751–2754.
- [4] C. L. M. Pereira, A. C. Doriguetto, C. Konzen, L. C. Meira-Belo, U. A. Leitao, N. G. Fernandes, Y. P. Mascarenhas, J. Elena, A. L. Brandl, M. Knobel, H. O. Stumpf, *Eur. J. Inorg. Chem.* **2005**, *24*, 5018–5025.
- [5] D. Cangussu, W. C. Nunes, C. L. M. Pereira, E. F. Pedroso, I. O. Mazali, M. Knobel, O. L. Alves, H. O. Stumpf, *Eur. J. Inorg. Chem.* **2008**, *24*, 3082–3808.
- [6] W. C. Nunes, L. M. Socolovsky, J. C. Denardin, F. Cebollada, A. L. Brandl, M. Knobel, *Phys. Rev. B* **2005**, *72*, 212413–212413-4.
- [7] a) E. Pardo, R. Ruiz-García, F. Lloret, J. Faus, M. Julve, Y. Journaux, F. S. Delgado, C. Ruiz-Pérez, *Adv. Mater.* **2004**, *16*, 1597–1600; b) E. Pardo, R. Ruiz-García, F. Lloret, J. Faus, M. Julve, Y. Journaux, M. A. Novak, F. S. Delgado, C. Ruiz-Pérez, *Chem. Eur. J.* **2007**, *13*, 2054–2066; c) E. Pardo, C. Train, R. Lescouëzec, Y. Journaux, J. Pasán, C. Ruiz-Pérez, F. S. Delgado, R. Ruiz-García, F. Lloret, C. Paulsen, *Chem. Commun.* **2010**, *46*, 2322–2324; d) J. Ferrando-Soria, E. Pardo, R. Ruiz-García, J. Cano, F. Lloret, M. Julve, Y. Journaux, J. Pasán, C. Ruiz-Pérez, *Chem. Eur. J.* **2011**, *17*, 2176–2188; e) J. Ferrando-Soria, D. Cangussu, M. Eslava, Y. Journaux, R. Lescouëzec, M. Julve, F. Lloret, J. Pasán, C. Ruiz-Pérez, E. Lhotel, C. Paulsen, E. Pardo, *Chem. Eur. J.* **2011**, *17*, 12482–12494.
- [8] a) E. Pardo, R. Ruiz-García, J. Cano, X. Ottenwaelde, R. Lescouëzec, Y. Journaux, F. Lloret, M. Julve, *Dalton Trans.* **2008**, *21*, 2769–2900; b) J.-M. Lehn, *Supramolecular Chemistry, Concepts and Perspectives*, Wiley-VCH, Weinheim, **1995**; c) G. R. Desiraju, *Nature* **2001**, *412*, 397–400.
- [9] a) S. Venkataramani, U. Jana, M. Dommaschk, F. D. Sönnichsen, F. Tuzcek, R. Herges, *Science* **2011**, *331*, 445–448; b) O. Kahn in *Molecular Magnetism: From Molecular Assemblies to the Devices* (Eds.: E. Coronado, P. Delhaes, D. Gatteschi, J. S. Miller), NATO ASI Series E321, Kluwer, Dordrecht, **1996**, pp. 243–288; c) M. Mannini, F. Pineider, P. Sainctavit, C. Danieli, E. Otero, C. Sciancalepore, A. M. Talarico, M.-A. Arrio, A. Cornia, D. Gatteschi, R. Sessoli, *Nat. Mater.* **2009**, *8*, 194–197.
- [10] M. T. Albelda, J. C. Frias, E. García-España, H.-J. Schneider, *Chem. Soc. Rev.* **2012**, *41*, 3859–3877.
- [11] a) J. S. Seo, D. Whang, H. Lee, S. I. Jun, J. Oh, Y. J. Jeon, K. Kim, *Nature* **2000**, *404*, 982–986; b) M. G. Speziali, F. C. C. Moura, P. A. Robles-Dutenhefner, M. H. Araujo, E. V. Gusevskaya, E. N. dos Santos, *J. Mol. Catal. A* **2005**, *239*, 10–14; c) W. Trakarnpruk, W. Kanjina, *Ind. Eng. Chem. Res.* **2008**, *47*, 964–968.
- [12] a) P. Starha, Z. Travnicek, I. Popa, *J. Inorg. Biochem.* **2009**, *103*, 978–988; b) B. Vernon-Cheney, D. J. Duchamp, R. E. Christoffersent, *J. Med. Chem.* **1982**, *26*, 719–725; c) S. Choi, A. B. Beeler, A. Pradhan, E. B. Watkins, J. M. Rimoldi, B. Tekwani, M. A. Aver, *J. Comb. Chem.* **2007**, *9*, 292–300.
- [13] F. J. Caires, L. S. Lima, C. T. Carvalho, A. B. Siqueira, O. Treu-Filho, M. Ionashiro, *J. Therm. Anal. Calorim.* **2012**, *107*, 335–344.

- [14] K. Nakamoto in *Infrared and Raman Spectra of Inorganic and Coordination Compounds, Part B: Applications in Coordination, Organometallic and Bioinorganic Chemistry*, 6th ed., Wiley, New York, **2009**, pp. 9–12, 79–82; P. X. Armendarez, K. Nakamoto, *Inorg. Chem.* **1966**, *5*, 796–800.
- [15] R. Kivekas, A. Pajune, A. Navarrete, E. Colacio, *Inorg. Chim. Acta* **1999**, *284*, 292–295.
- [16] B. Cervera, J. L. Sanza, M. J. Ibáñez, G. Vila, F. Lloret, M. Julve, R. Ruiz, X. Ottenwaelder, A. Aukauloo, S. Poussereau, Y. Journaux, M. Carmen-Muñoz, *J. Chem. Soc., Dalton Trans.* **1998**, 781–790.
- [17] a) I. Dance, M. Scudder, *Chem. Eur. J.* **1996**, *2*, 481–486; b) I. Dance, M. Scudder, *J. Chem. Soc., Dalton Trans.* **1996**, 3755–3769; c) M. Scudder, I. Dance, *J. Chem. Soc., Dalton Trans.* **1998**, 3155–3165.
- [18] a) S. A. O’Kane, R. Clerac, H. Zhao, X. Ouyang, J. R. Galán-Mascarós, R. Heintz, K. Dunbar, *J. Solid State Chem.* **2000**, *152*, 159–173; b) J. H. Liao, F. Leroux, C. Payen, D. Guyomard, Y. Piffard, *J. Solid State Chem.* **1996**, *121*, 214–224; c) Y. Matsunaga, F. Nakamura, H. Takahashi, T. Hashimoto, *Solid State Commun.* **2008**, *145*, 502–506; d) F. Nakamura, Y. Matsunaga, N. Ohba, K. Arai, H. Matsubara, H. Takahashi, T. Hashimoto, *Thermochim. Acta* **2005**, *435*, 222–229; e) K. Oikawa, T. Ota, Y. Sutou, T. Ohmori, R. Kainuma, K. Ishida, *Mater. Trans.* **2002**, *43*, 2360–2362; f) R. Gheorghie, M. Kalisz, R. Clérac, C. Mathonière, P. Herson, Y. Li, M. Seuleiman, R. Lescouëzec, F. Lloret, M. Julve, *Inorg. Chem.* **2010**, *49*, 11045–11056.
- [19] a) J. Sletten, H. Hope, M. Julve, O. Kahn, M. Verdagner, A. Dworkin, *Inorg. Chem.* **1988**, *27*, 542–549; b) D. Armentano, G. De Munno, T. F. Mastropietro, M. Julve, F. Lloret, *J. Am. Chem. Soc.* **2006**, *127*, 10778–10779; c) D. Armentano, F. Mastropietro, G. De Munno, P. Rossi, F. Lloret, M. Julve, *Inorg. Chem.* **2008**, *47*, 3772–3786.
- [20] R. L. Carlin in *Magnetochemistry*, Springer, Berlin, **1986**.
- [21] F. Lloret, M. Julve, J. Cano, R. Ruiz-García, E. Pardo, *Inorg. Chim. Acta* **2008**, *361*, 3432–3445.
- [22] a) M. E. Lines, *J. Chem. Phys.* **1971**, *55*, 2977–2984; b) G. De Munno, M. Julve, F. Lloret, J. Faus, A. Caneschi, *J. Chem. Soc., Dalton Trans.* **1994**, 1175–1183; c) G. De Munno, T. Porerio, M. Julve, F. Lloret, G. Viau, *New J. Chem.* **1998**, *22*, 299–305; d) S. O. H. Guntschke, D. J. Price, A. K. Powell, P. T. Wood, *Eur. J. Inorg. Chem.* **2001**, 2739–2741; e) C. Ruiz-Pérez, P. Lorenzo-Luis, M. Hernández-Molina, M. Milagros-Laz, F. S. Delgado, P. Gili, M. Julve, *Eur. J. Inorg. Chem.* **2004**, 3873–3879; f) V. Mishra, F. Lloret, R. Mukherjee, *Inorg. Chim. Acta* **2006**, *359*, 4053–4062; g) O. Fabelo, J. Pasán, F. Lloret, M. Julve, C. Ruiz-Pérez, *CrystEngComm* **2007**, *9*, 815–827; h) O. Fabelo, J. Pasán, L. Cañadillas-Delgado, F. S. Delgado, A. Labrador, F. Lloret, M. Julve, C. Ruiz-Pérez, *Cryst. Growth Des.* **2008**, *8*, 3984–3992; i) O. Fabelo, J. Pasán, M. Julve, C. Ruiz-Pérez, *Inorg. Chem.* **2008**, *47*, 3568–3576; j) O. Fabelo, J. Pasán, L. Cañadillas-Delgado, F. S. Delgado, F. Lloret, M. Julve, C. Ruiz-Pérez, *Inorg. Chem.* **2008**, *47*, 8053–8061; k) O. Fabelo, J. Pasán, L. Cañadillas-Delgado, F. S. Delgado, C. Yuste, F. Lloret, M. Julve, C. Ruiz-Pérez, *CrystEngComm* **2009**, *11*, 2169–2179; l) O. Fabelo, J. Pasán, L. Cañadillas-Delgado, F. S. Delgado, F. Lloret, M. Julve, C. Ruiz-Pérez, *Inorg. Chem.* **2009**, *48*, 6086–6095; m) F. S. Delgado, C. A. Jiménez, P. Lorenzo-Luis, J. Pasán, O. Fabelo, L. Cañadillas-Delgado, F. Lloret, M. Julve, C. Ruiz-Pérez, *Cryst. Growth Des.* **2012**, *12*, 599–614.
- [23] a) Y. Journaux, J. Sletten, O. Kahn, *Inorg. Chem.* **1986**, *25*, 439–447; b) R. Ruiz, M. Julve, J. Faus, F. Lloret, M. C. Munoz, Y. Journaux, C. Bois, *Inorg. Chem.* **1997**, *36*, 3434–3439; c) E. A. Buvaylo, V. N. Kokozay, O. Y. Vassilyeva, B. W. Skelton, J. Jezierska, L. C. Brunel, A. Ozarowski, *Chem. Commun.* **2005**, 4976–4978; d) P. Chaudhuri, M. Winter, B. P. C. D. Védova, E. Bill, A. Trautwein, S. Gehring, P. Fleischhauer, B. Nuber, J. Weiss, *Inorg. Chem.* **1991**, *30*, 2148–2157.
- [24] L. C. A. Oliveira, M. F. Portilho, A. C. Silva, H. A. Taroco, P. P. Souza, *Appl. Catal. B* **2012**, *117–118*, 29–35.
- [25] H. O. Stumpf, Y. Pei, O. Kahn, J. Sletten, J. P. Renard, *J. Am. Chem. Soc.* **1993**, *115*, 6738–6745.
- [26] Xcalibur CCD system, *Agilent Technologies: CrysAlisPro Software system*, version 1.171.35.15, Agilent Technologies UK Ltd, Oxford, **2011**.
- [27] L. Palatinusz, G. Chapuis, *J. Appl. Crystallogr.* **2007**, *40*, 786–790.
- [28] G. M. Sheldrick, *SHELXL-97, Program for Crystal Structure Refinement*, University of Göttingen, Göttingen, **1997**.
- [29] L. J. Farrugia, *J. Appl. Crystallogr.* **1997**, *30*, 565–566.

Received: July 24, 2012

Published Online: October 11, 2012